Flow and clog in a silo with oscillating exit

Kiwing To* and Hsiang-Ting Tai
Institute of Physics, Academia Sinica, Taipei 115, Taiwan
(Received 26 May 2017; published 14 September 2017)

When grains flow out of a silo, flow rate W increases with exit size D. If D is too small, an arch may form and the flow may be blocked at the exit. To recover from clogging, the arch has to be destroyed. Here we construct a two-dimensional silo with movable exit and study the effects of exit oscillation (with amplitude A and frequency f) on flow rate, clogging, and unclogging of grains through the exit. We find that, if exit oscillates, W remains finite even when D (measured in unit of grain diameter) is only slightly larger than one. Surprisingly, while W increases with oscillation strength $\Gamma \equiv 4\pi^2 A f^2$ as expected at small D, W decreases with Γ when $D \geqslant 5$ due to induced random motion of the grains at the exit. When D is small and oscillation speed $v \equiv 2\pi A f$ is slow, temporary clogging events cause the grains to flow intermittently. In this regime, W depends only on v—a feature consistent to a simple arch breaking mechanism, and the phase boundary of intermittent flow in the D-v plane is consistent to either a power law: $D \propto v^{-7}$ or an exponential form: $D \propto e^{-D/0.55}$. Furthermore, the flow time statistic is Poissonian whereas the recovery time statistic follows a power-law distribution.

DOI: 10.1103/PhysRevE.96.032906

I. INTRODUCTION

Silos and hoppers are common industrial and agricultural appliances for transporting or distributing granular materials. The flow of granular materials through these appliances is controlled (or limited) by the exit. Clearly the exit size is the most important factor that determines the outflow rate [1–6] while the pressure seems to play a minor role [7,8]. For a three-dimensional silo with grain of average diameter d, the empirical relationship: $W \propto (D-k)^{5/2}$ between flow rate W and exit size D (in unit of d) has been reported more than 50 years ago by Beverloo [9] and it has been widely accepted for $D \gg 1$ until recently [10]. In principle, Beverloo Law breaks down for small D when the flow is clogged stochastically [2–6]. In this regime no continuous flow can be sustained without external means to recover from clogging events.

In fact the cause of a clog event is known—formation of an arch in two-dimensional silo (or a dome in three dimension) with size larger than the bottle neck [2] at the outlet. For granular flow to be clogged, not only that an arch has to be formed, the arch that blocks the flow has to be strong enough to withstand perturbation due to motion of the grains above the arch before all grains motions are stopped [11]. Hence, there are devices (such as vibrator [12], air cannons, etc.) invented to tackle the problem. Although the working principle of these devices is rather simple: prevent formation of the arch that blocks the flow and breaks the arch once it is formed, there is not yet a satisfactory way to avoid clogging completely [13–15]. For example, if the hopper is vibrated, the perturbation due to the vibration may destabilize the arch that clogs the flow as suggested in the experiments by Lozano *et al.* [16]. However, vibrating the whole hopper requires a big machine which is very probably an energy hog. Intuitively, if any one of the two bases of the clog forming arch is loosened in a two-dimensional silo, the arch will break. To test this simple idea, we build a two-dimensional silos with beads flowing out through an outlet that oscillates perpendicular to the flow direction.

Using silos with movable exit and an electronic balance for flow rate measurement, we find that finite flow rate can be sustained by the motion of the exit even when the exit size is just slightly larger than the grain diameter. Furthermore, while the flow rate W increases with oscillation strength as expected at small exit size D, W decreases with oscillation strength when $D \geqslant 5$ and the values of W can be collapsed on a straight line with respect to an effective variable $\xi \equiv W_o(D-k)^{3/2} - a(D-5)\Gamma$. Here, $\Gamma \equiv 4\pi^2 A f^2$ is the typical acceleration of exit oscillation, A and f are, respectively, the amplitude and frequency of oscillation. In this regime, arch does not form readily so that beads flow continuously through the exit. The motion of the exit induces random motion of the beads at the exit so that W decreases. On the other hand, when D is reduced, we observe a change from continuous flow to an intermittent flow regime in which temporary clogging events occur stochastically. In this regime, the flow rate, which depends on both A and f for a silo of exit size D, can be collapsed by plotting against the typical oscillation speed $v \equiv 2\pi A f$. Hence, the flow rate is a function of v only—a feature consistent with a simple physical mechanism related to the motion of the exit.

In the intermittent flow regime, we also find that the flow time t_f before clogging is exponentially distributed [3,15,17]. In particular, the reliability function [18] $P(t_f)$ is found to be proportional to $\exp(-t_f/\langle t_f\rangle)$, an expected feature of Poisson processes for random and independent clogging events. On the other hand, the statistics of the recovery time t_r (defined as the time from clog to flow [14]) is power-law distributed: $P(t_r) \propto t_r^{-\alpha}$ with $\alpha = 2.25$. This suggests that the packing above the exit may be driven to a self-organized critical state [19] before the arch at the exit is broken by the oscillation which acts as perturbations. Moreover, the value of α, being greater than unity, implies that the average recovery time remains finite. This result contributes another evidence for sustainable finite flow rate due to exit oscillation.

*ericto@gate.sinica.edu.tw

 ©2017 American Physical Society

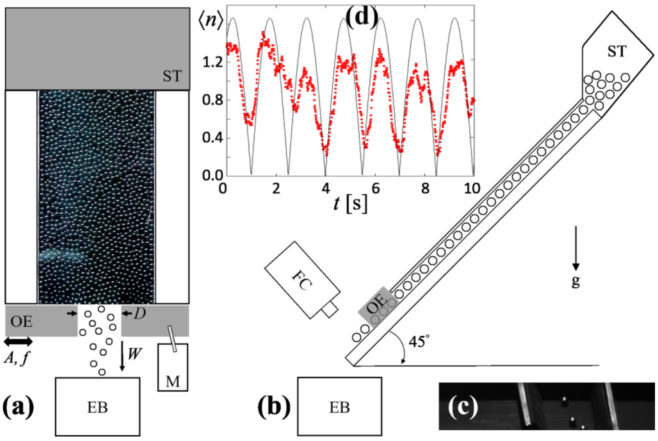

FIG. 1. Experimental setup: (a) front view and (b) side view. ST: storage tank, oscillating exit, M: motor with crankshaft (M), EB: electronic balance, FC: fast camera. (c) A typical image from FC. (d) Average bead number $\langle n\rangle$ in an image (red dots). The black trace represents the instantaneous speed of the exit.

II. EXPERIMENT

A two-dimensional silo with a storage tank (ST) on top is constructed using an aluminum plate and a glass plate as the walls with two acrylic spacers in between as shown in Fig. 1(a) and (b). The dimension of the glass plate is $60 \times 50\ \mathrm{cm}^2$ while the acrylic spacers, which are $60 \times 13\ \mathrm{cm}^2$ and 3.3 mm thick, are placed 24 cm apart. Hence, we have a silo of internal dimension $60 \times 24\ \mathrm{cm}^2 \times 3.3$ mm. Metal beads of 3 mm diameter and weight 0.11 g are loaded in the silo through the storage tank on top. Since the space between the walls are only slight larger than the bead diameter, the beads inside the silo are packed in one single layer. The bottom of this thin silo is made of two aluminum blocks that are mounted on a pair of linear rails so that a movable outlet of adjustable exit size D is constructed.

A metal rod with ball joint bearings at both ends is used to link the outlet block to a homemade crankshaft which is driven by a DC-motor (M). In this way, the exit of the silo can oscillate horizontally with well-controlled oscillation strength characterized by the typical speed $v \equiv 2\pi Af$ and acceleration $\Gamma \equiv A(2\pi f)^2$, where A and f are the oscillation amplitude and the frequency, respectively. The typical acceleration Γ will be expressed in unit of $9.81\ \mathrm{m/s}^2$, the acceleration due to gravity.

The silo is mounted on a platform inclined at 45° from the vertical direction. A digital electronic balance (EB) running at 5.5 measurements per second is placed below the outlet to measure the average flow rate (W) of the beads from the silo. A fast video camera (FC) with 1 ms exposure time running at 100 frame per second is installed to capture images of the beads that flow out of the silo. Figure 1(c) is a typical image captured by the camera at $D = 2.08$, $A = 33$ mm, and $f = 0.33$ Hz. The number of beads n in the image can be obtained by standard imaging software. If $n = 0$ for longer than 0.04 s, which is the time for a beads to fall a distance of its diameter from rest, the silo is considered clogged. Furthermore the average bead number $\langle n\rangle$, calculated by a running average filter of 0.3 s time window, is found to be highly correlated to the instantaneous speed of the exit at small flow rate as shown in Fig. 1(d). Hence the typical speed v of the exit may be a good physical quantity to analyses the flow rate data at small exits.

III. RESULTS AND DISCUSSIONS

A. Flow rate for silo with large exits

Figure 2 shows the flow rate data from the electronic balance. The black dots in Fig. 2(a) are the measurement obtained at oscillation amplitude $A = 7.6$ mm and frequency $f = 3.3$ Hz so that $\Gamma = \Gamma_o = 0.34$. The line through the dots in the figure is a fitted curve using the Beverloo Law: $W = W_o(D-k)^{3/2}$, where $W_o = 3.07 \pm 0.03$ g/s and $k = 0.68 \pm 0.04$. Apparently the flow curve at this oscillation condition obeys the Beverloo Law with exit size down to about two times the bead diameter. However, the flow rate of a fixed exit size varies with the oscillation strength as demonstrated by the red '×' for $\Gamma < \Gamma_o$ and blue '+' for $\Gamma > \Gamma_o$ in the figure. Roughly speaking, for silos of small exit sizes ($D \lesssim 5$), flow rate increases with oscillation strength. On the other hand, W decreases with Γ for silos of large D. Although the reduction of discharge rate from a horizontally vibrated silo had been reported by Hunt *et al.* [20], the physical mechanism for flow reduction due to exit oscillation was not clear.

It should be pointed out that if the exit is not oscillating, W vanishes when D is close to 5 due to formation of a permanent arch above the exit [2]. Similar to the tilted silo experiments by Thomas and Durian [5], there is no signature of clogging transition at $D \approx 5$ in our experiments. However, unlike the experiments performed in ref. [5] in which flow was recovered from a clogged configuration by breaking the blocking arch manually, finite flow rate can be sustained by exit oscillation in our experiments with exit size down to 1.27 time the bead diameter. Hence, one can indeed keep the silo running without clogging by exit oscillation, albeit with small flow rate. When flow rate W is plotted against the acceleration Γ of exit oscillation at a fixed exit size for $D \gtrsim 5$, a linear relation: $W = -a\Gamma + b$ is revealed [see inset of Fig. 2(a)]. The rate a at which W decreases with Γ is found to increase with exit size D such that $a = c(D-5)$ with $c = 1.6 \pm 0.1$ g/s. This implies that the effect of Γ on W is stronger at larger exit size.

We believe at large exit size, the flow is fast and the beads near the exit are fluidized. Hence, no arch can be formed. If the exit is not oscillating, a continuous stream of beads flow out of the exit with velocities mainly directed downward as shown in Fig. 3(a). Only the beads close to the edge of the exit have better chance to hit the edge and acquire significant horizontal speed. However, when the exit is oscillating, collisions between the beads and the edge of the exit give the beads horizontal speeds that may lead to collisions among the beads before they fall through the exit. Hence the kinetic stress [21] of the granular fluid at the exit increases and the flow rate is reduced. Intuitively, if the collisions are strong enough a bead may even moves upward as illustrated in Fig. 3(b). Since the impulse on the beads increases with the relative velocity between the exit edge and the colliding beads, the reduction of flow rate will be larger at larger exit size when the average flow speed of the beads are larger. This mechanism of flow rate reduction due to oscillation at large exit size suggests a possible effective

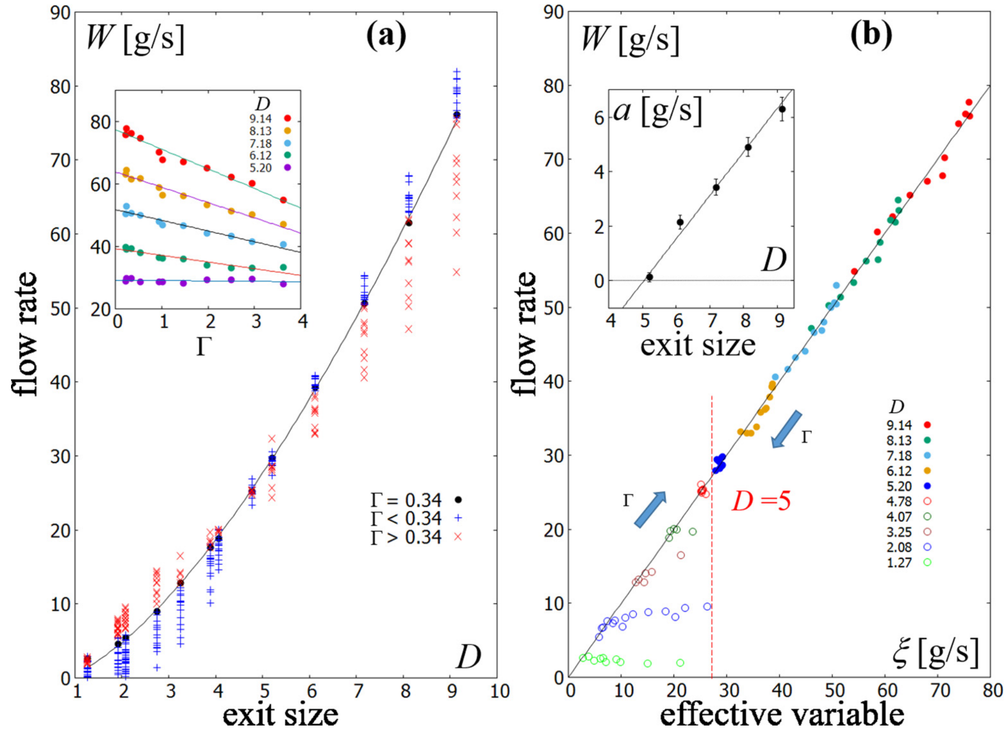

FIG. 2. (a) Flow rate W versus exit size D at different oscillation acceleration Γ. The line through the black dots is the least square fit of the Beverloo Law to the data $\Gamma = 0.34$. Inset shows the effect of Γ on W at different D. (b) W versus the effective variable $\xi \equiv W_o(D-k)^{3/2} - c(D-5)\Gamma$. The vertical dashed red line corresponds to $D = 5$ and the arrows indicate the directions of increasing Γ. Inset shows the linear relationship between the rate a of decreasing W with respect to Γ from which the quantity c via $a = c(D-5)$ is obtained.

variable $\xi \equiv W_o(D-k)^{3/2} - c(D-5)\Gamma$ through which the flow rate data should be collapsed. This particular form for the effective variable is consistent to our experimental observation and it reduces to the Beverloo Law when the exit is not vibrating. Figure 2(b) is the plot of W versus ξ. One can see that this ansatz performs satisfactorily for $D > 5$ but not so for $D < 5$.

Although W does not collapse well for small D, they approach the collapse curve at large Γ. Presumably the strong oscillation of the exit prevents the formation of the arch at the exit and hence the arguments in the previous paragraph are applicable. Nevertheless, the scattering of the data for small D implies that Γ is not a good physical quantity to analyze the data. The strong correlation between the average number of beads $\langle n \rangle$ and the instantaneous speed of the exit [see Fig. 1(d)] suggests that the exit oscillation speed $v \equiv 2\pi Af$ may be a better parameter to understand the physics in this regime.

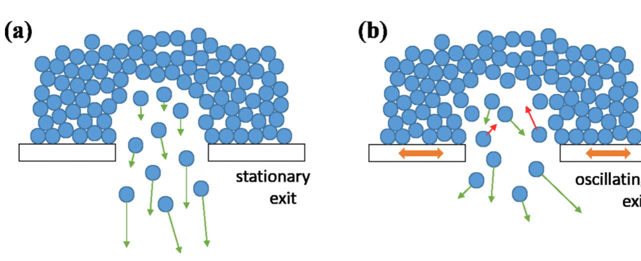

FIG. 3. Schematic diagrams illustrating the velocities of the beads near the exit when the exit is (a) stationary and (b) oscillating.

B. Flow rate for silo with small exits

The reason of the unsatisfactory data collapse in the small exit regime using Γ may arise from the deviation from Beverloo Law. This can be checked by plotting $W^{2/3}$ against D [see Fig. 4(a)]. The results confirms that flow rate does deviate from the Beverloo Law in small D. Under certain oscillation strength the dependence $W \sim (D-k)^{3/2}$ is valid down to $D \gtrsim 2$. At other oscillation strength, $W(D)$ deviates from the three-half power-law when D is smaller that a certain value D_c. When we examine the temporal record of the reading $m(t)$ from the electronic balance for the experiment conducted at small oscillation ($A = 2.0\,\mathrm{mm}$, $f = 0.17\,\mathrm{Hz}$) and small $D(=2.75)$, we find plateaus that signify the presence of temporary clogging events as shown in Fig. 4(b). These clogging events cause the flow to be intermittent and it can indeed be observed visually. Transition from continuous flow to intermittent flow by reducing the exit size at constant oscillation strength can also be observed when the oscillation strength is reduced at constant exit size.

C. Intermittent flow

In the intermittent flow regime, beads flow out of the silo for a time period t_f before a clogging event that stops the flow momentarily. Then after a recovery time period t_r, beads start to flow again as illustrated by Fig. 4(b). Since the data rate of electronic balance is slow, we use the images from the fast camera to measure t_f and t_r with a better temporal resolution. We consider that if there is no bead captured in four consecutive frames (i.e., a period of 0.04 s which is the

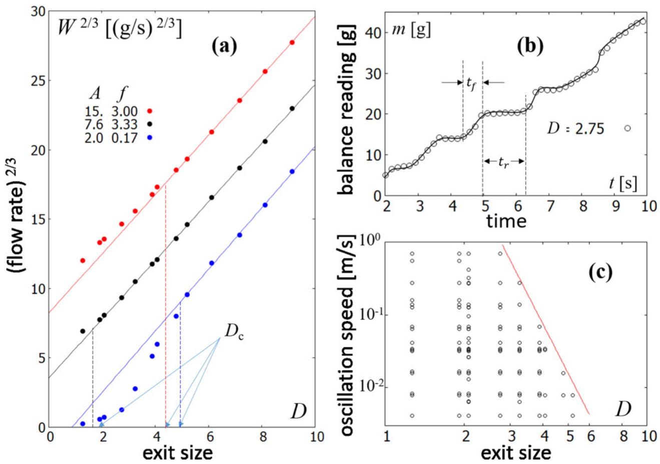

FIG. 4. (a) Two-third power of average flow rate $W^{2/3}$ versus exit size D at different oscillation amplitude A and frequency f. To separate the data for better viewing, data values for $A = 7.6$ mm (black dots, $\Gamma = 0.34$) are shifted up by 5 units and those for $A = 15$ mm (red dots, $\Gamma = 0.53$) are shifted up by 10 units. (b) Time variation of the reading from electronic balance for $D = 2.75$ obtained at $A = 2.0$ mm and $f = 0.17$ Hz. (c) Phase diagram for intermittent flow in the v-D plane. The phase boundary between intermittent and continuous flows in the figure can be fitted to a power law: $v \sim D^{-7}$ and equally well to an exponential form: $v \sim e^{-D/0.55}$.

time for a bead to move a distance of its diameter from rest), it is within a temporary clogging event. Otherwise, it is in the flow state. In this way, we can identify the oscillation conditions, characterized by the oscillation speed $v \equiv 2\pi A f$, for intermittent flow in silo of exit size D as shown in Fig. 4(c). Interestingly, the phase boundary for the intermittent flow seems to follow either a power law: $v \sim D^{-7}$ or an exponential form: $v \sim e^{-D/0.55}$. Extrapolation of the phase boundary to vanishing v (i.e., stationary exit) would imply the absence of a finite exit size [4,6,17] beyond which clogging is impossible.

D. Flow time and recovery time in intermittent flow regime

In previous studies of silo with stationary exit, the transition from clogging to continuous flow is accompanied by rapid increase of avalanche size [4,6,17] which is defined as the amount of material that go through the exit before clogging occurs. In our experiments, in which finite flow rate can be sustained, the equivalent avalanche size is proportional to the flow time t_f in intermittent flow regime. Figure 5(a) shows that when the exit oscillation speed is small ($v \lesssim 0.1$ m/s), the average flow time $\langle t_f \rangle$ grows exponentially with D such that $\langle t_f \rangle = t_0 e^{D/D_0}$ with $t_0 = 1.69 \times 10^{-2}$ s and $D_0 = 1.89$. At strong exit oscillation [e.g., $v = 0.159$ m/s in Fig. 5(a)] $\langle t_f \rangle$ grows faster than exponentially. Obviously, $\langle t_f \rangle$ diverges when approaching the boundary of intermittent to continuous flow transition. In this situation, the upper bound of $\langle t_f \rangle$ is set by the duration of the experiment. In an experiment that lasts for a time period T in which the total flow time is T_f, the duty cycle $\phi \equiv T_f/T$, which approximates the probability of finding the silo at a particular moment, is more informative. The inset of Fig. 5(a) shows that ϕ increases with D and becomes unity when $D \gtrsim 5$, as expected.

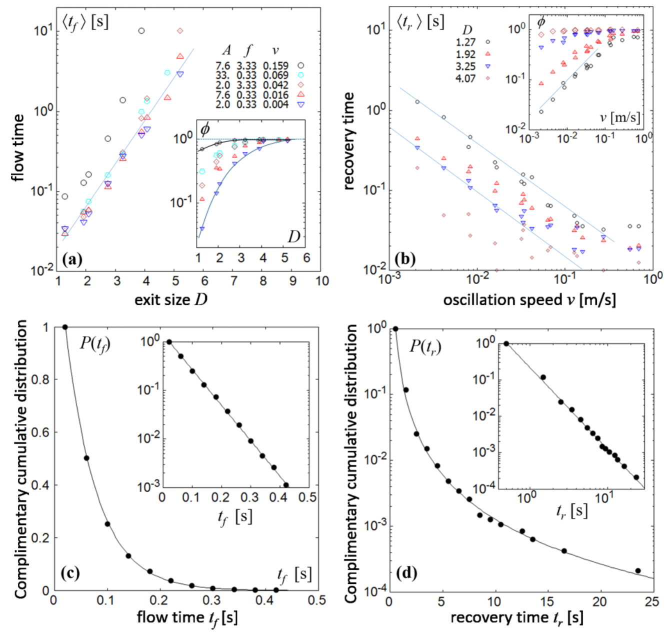

FIG. 5. (a) Variation of average flow time $\langle t_f \rangle$ with exit size D at different oscillation parameters. Inset shows the change of duty cycle ϕ with D. The lines in the graphs are guide to the eye. (b) Variation of average recovery time $\langle t_r \rangle$ with oscillation speed v at different D. The lines has slope equals -0.75. Inset shows how ϕ varies with v. The slope of the line in the inset is 0.6. (c) Complementary cumulative distribution $P(t_f)$ of flow time t_f at $A = 1.56$ mm, $f = 0.33$ Hz, and $v = 3.3 \times 10^{-3}$ m/s when $D = 2.08$. Inset: Same data plotted in semi-logarithmic graph with the fitted curve: $P(t_f) = 1.4 \exp(-t_f/0.059)$. (d) Complementary cumulative distribution $P(t_r)$ of recovery time t_r at the same oscillation condition is plotted in semi-logarithmic scale. Inset: Same data plotted double logarithmic graph with the fitted line: $P(t_r) = 0.22 t_r^{-2.25}$.

While the average flow time is a measure of how often one has to wait before a temporary clog occurs due to formation of an arch at the exit, the average recovery time $\langle t_r \rangle$ indicates how long the arch persists under the influence of the motion of the exit. Clearly, the faster the exit moves, the faster the arch should break. Hence $\langle t_r \rangle$ should decreases with v whereas the duty cycle should increases with v. Figure 5(b) shows that $\langle t_r \rangle$ decreases with oscillation speed v approximately in a power-law: $\langle t_r \rangle \sim v^{-0.75}$ when $D < 4$. On the other hand, the duty cycle increases approximately with $v^{0.6}$.

The difference in functional dependence of $\langle t_f \rangle$ on D and $\langle t_r \rangle$ on v suggests a fundamental differences between clogging and clog recovery processes. Since the transition from flow to clog and that from clog to flow are stochastic processes, one can measure the the probability density $p(t_f)$ and calculate the reliability function, or complementary cumulative distribution, $P(t_f) \equiv \int_{t_f}^{\infty} p(\tau) d\tau$. Figure 5(c) is the graph of $P(t_f)$ for a silo with $D = 2.08$, $A = 7.6$ mm, and $f = 0.33$ Hz. The inset in this graph implies $P(t_f) \sim \exp(-t_f/\langle t_f \rangle)$, an exponential decay function which is typically found in Poisson process with a constant transition rate [15]. Hence, the clogging transition is related to the spontaneous formation of an arch at the exit. In contrast, the complementary cumulative distribution $P(t_r)$ obtained for the recovery time in the same experiment is a power-law function $P(t_r) \sim t_r^{-\alpha}$ with $\alpha = 2.25$ as shown in Fig. 5(d). Power-law probability density for the waiting time distribution is usually related to self organize criticality [19,22] that underlying earthquake in which stresses are built up before the onset. The breaking of the arch at the end of the recovery period in our experiment may be analogous to the onset of earthquake. During the recovery period, horizontal motion of the exit introduces rearrangement of the packing above the arch it is deformed to an unstable configuration and breaks [11,16].

Note that the value of α is greater than 2. So the probability density, which is proportional to the derivative of $P(t_r)$, will decrease faster than the inverse third power of t_r. Let the minimal value of t_r be t_o which is determined by the experimental method. Then the average recovery time $\langle t_r \rangle \propto \int_{t_0}^{\infty} \tau^{-\alpha} d\tau$ is finite. Since a permanent clog will cause $\langle t_r \rangle$ to diverge, the above analysis implies that the clogging events in our experiments are always temporary and hence finite flow rate can be sustained indefinitely.

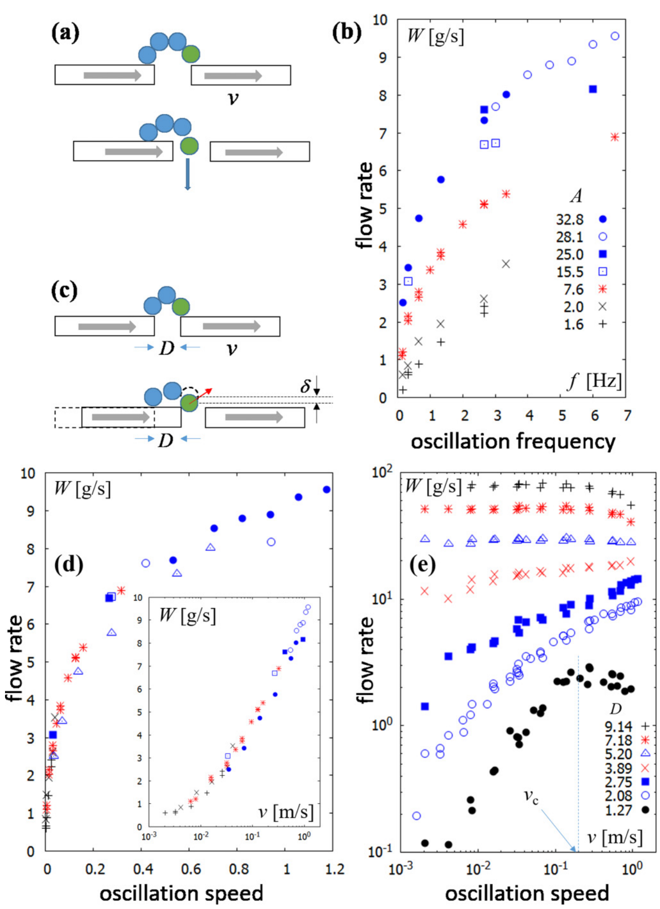

FIG. 6. (a) Schematic diagram of the bead at the base of an arch falling out when the exit moves. (b) Flow rate W versus oscillation frequency f at different oscillation amplitude A measured at $D = 2.08$. (c) Schematic diagram of the bead being hit by the edge of the exit with an upward impulse if δ is less than the radius of the bead. (d) Same data in (b) when plotted against oscillation speed v for different combinations of oscillation amplitude A and frequency f when the exit size $D = 2.08$. The inset shows the quality of data collapse for small v. (e) W versus v in double logarithmic plot for different D.

E. Arch breaking mechanism

In the intermittent flow regime, the presence of temporary clogs implies the failure of arch prevention by exit oscillation. Nevertheless even when an arch is formed, it may be broken by the motion of the exit. Figure 6(a) illustrates one possible mechanism for the breaking of an arch. When the exit moves to the base (green) of an arch, the base falls out through the exit. Hence the arch will fall apart and flow will resume. If this mechanism is responsible for the flow, the flow rate should increase with the oscillation speed. Figure 6(b) shows the variation of the flow rate with oscillation frequency f at different oscillation amplitude A for the silo of exit size $D = 2.08$. While W depends on both f and A, the flow data collapse on a single curve when plotted against oscillation speed v [see Fig. 6(a) and its inset]. Similar data collapse of the flow rate for silos of different exit size are also observed as shown in Fig. 6(b). Hence, instead of depending on two independent parameters A and f, W at a particular exit size is a function of v only.

Note that W starts to decrease with v when $v > 0.2$ m/s for the silo with the smallest exit ($D = 1.27$) as shown in Fig. 6(b). To explain this observation, we consider the scenario depicted in Fig. 6(c). Consider a bead starts to fall from rest near the exit and hit by the edge of the exit after falling a distance δ. If δ is less than the radius r of the bead, the bead will acquire an upward impulse from collision and W will be reduced. The speed v_c at which this happens can be estimated by $\frac{1}{2} g \sin 45^\circ (2Dr/v_c)^2 \leqslant r$. This leads to $v_c \geqslant 0.28$ m/s, which is consistent to our data as shown in Fig. 6(d).

IV. SUMMARY

To summarize, we investigate granular flow of mono-disperse beads out of a two-dimensional silo with an oscillating exit. Because of exit oscillation, finite flow rate can be sustained beyond the clogging transition that occurs for stationary exit at exit size approximately five times the grain size. Although Beverloo Law is found to be valid beyond the clogging transition due to exit oscillation, the effect of exit oscillation on flow rate is very different for silos with large and small exit sizes.

Conceptually, exit size represents the geometrical aspect that determines how readily arches are formed at the silo exit while exit oscillation is a dynamical effect that determines how effective the formation of arches are prevented and how fast the arches are destroyed by the motion of the exit. For silo with large exit size, arch formation is not possible, exit oscillation makes no positive contribution to flow rate. Instead it induces random motion of the beads and hence increases the resistance to the flow. At small exit sizes when arches are formed readily, these arches slow down the flow and may even block the flow in a silo with stationary exit. Under exit oscillation, arch formation may be completely prevented and hence continuous flow is possible and flow rate increases with oscillation strength. For silos with even smaller exits, arch formation cannot be avoided even with exit oscillation and the flow in the silo will be blocked. Nevertheless, when the flow is blocked, the motion of the exit serves to destroy the arch by loosening one of the bases of the arch and the flow may resume. These temporary clogging events cause the beads to flow intermittently with flow rate depends only on the oscillation speed according to the arch breaking mechanism proposed.

Finally, we find that the probability density of the flow time and recovery time are, respectively, exponential and power-law distributed, implying fundamental differences in the physical processes of clogging and unclogging. Currently we are building three-dimensional silos to check if the flow behave differently to those of the two-dimensional silos. We believe our studies will not only enhance the basic understanding of the physics of clogging and unclogging but also lead to a better designs of devices and appliances [12,23] for transporting or distributing granular materials without clogging.

ACKNOWLEDGMENTS

The authors would like to thank Prof. D. Durian for his comments about Beverloo Law in granular flow in three-dimensional silos, Miss Ya-Chin Chen for her help as a summer intern during the preliminary stage of the project, and Dr. Chi-Keung Chan for his valuable suggestions about the manuscript. This work is supported by the Ministry of Science and Technology R.O.C. (104-2112-M-001-046).

[1] I. Zuriguel, D. R. Parisi, R. C. Hidalgo, C. Lozano, A. Janda, P. A. Gago, J. P. Peralta, L. M. Ferrer, L. A. Pugnaloni, E. Clément, D. Maza, I. Pagonabarraga, and A. Garcimartin, Sci. Rep. **4**, 7324 (2014).
[2] K. To, P.-Y. Lai, and H. K. Pak, Phys. Rev. Lett. **86**, 71 (2001).
[3] I. Zuriguel, L. A. Pugnaloni, A. Garcimartin, and D. Maza, Phys. Rev. E **68**, 030301 (2003).
[4] I. Zuriguel, A. Garcimartin, D. Maza, L. A. Pugnaloni, and J. M. Pastor, Phys. Rev. E **71**, 051303 (2005).
[5] C. C. Thomas and D. J. Durian, Phys. Rev. E **87**, 052201 (2013).
[6] C. C. Thomas and D. J. Durian, Phys. Rev. Lett. **114**, 178001 (2015).
[7] M. A. Aguirre, R. De Schant, and J.-C. Géminard, Phys. Rev. E **90**, 012203 (2014).
[8] M. A. Aguirre, J. G. Grande, A. Calvo, L. A. Pugnaloni, and J.-C. Géminard, Phys. Rev. Lett. **104**, 238002 (2010).
[9] W. A. Beverloo, H. A. Leniger, and J. van de Velde, Chem. Eng. Sci. **15**, 260 (1961).
[10] A. Janda, I. Zuriguel, and D. Maza, Phys. Rev. Lett. **108**, 248001 (2012).
[11] K. To and P.-Y. Lai, Phys. Rev. E **66**, 011308 (2002).
[12] T. H. Kollmann and J. Tomas, Part. Sci. Technol. **20**, 15 (2002).
[13] I. Zuriguel, A. Janda, A. Garcimartin, C. Lozano, R. Arevalo, and D. Maza, Phys. Rev. Lett. **107**, 278001 (2011).
[14] A. Janda, D. Maza, A. Garcimartin, E. Kolb, J. Lanuza, and E. Clément, Europhys. Lett. **87**, 24002 (2009).
[15] C. Mankoc, A. Garcimartin, I. Zuriguel, D. Maza, and L. A. Pugnaloni, Phys. Rev. E **80**, 011309 (2009).
[16] C. Lozano, G. Lumay, I. Zuriguel, R. C. Hidalgo, and A. Garcimartin, Phys. Rev. Lett. **109**, 068001 (2012).
[17] K. To, Phys. Rev. E **71**, 060301 (2005).
[18] C. Ebeling, *An Introduction to Reliability and Maintainability Engineering*, 2nd ed. (Waveland Press, Long Grove, IL, 2010).
[19] P. Bak and M. Paczuski, Proc. Natl. Acad. Sci. **92**, 6689 (1995).
[20] M. L. Hunt, R. C. Weathers, A. T. Lee, C. E. Brennen, and C. R. Wassgren, Phys. Fluids **11**, 68 (1999).
[21] S. M. Rubio-Largo, A. Janda, D. Maza, I. Zuriguel, and R. C. Hidalgo, Phys. Rev. Lett. **114**, 238002 (2015).
[22] K. Christensen, L. Danon, T. Scanlon, and P. Bak, Proc. Natl. Acad. Sci. **99**, 2509 (2002).
[23] P. Wen, N. Zheng, J. Nian, L. Li, and Q. Shi, Sci. Rep. **5**, 9880 (2015).